

Nuclear suppression of dileptons at forward rapidities

This content has been downloaded from IOPscience. Please scroll down to see the full text.

2011 J. Phys.: Conf. Ser. 312 022011

(<http://iopscience.iop.org/1742-6596/312/2/022011>)

View [the table of contents for this issue](#), or go to the [journal homepage](#) for more

Download details:

IP Address: 192.17.211.103

This content was downloaded on 03/11/2015 at 23:30

Please note that [terms and conditions apply](#).

Nuclear suppression of dileptons at forward rapidities

J. Čepila¹ and J. Nemchik^{1,2}

¹ Czech Technical University in Prague, FNSPE, Břehová 7, 11519 Prague, Czech Republic

² Institute of Experimental Physics SAS, Watsonova 47, 04001 Košice, Slovakia

E-mail: jan.cepila@fjfi.cvut.cz; nemchik@saske.sk

Abstract. Data from E772 and E866 experiments on the Drell-Yan process exhibit a significant nuclear suppression at large Feynman x_F . We show that a corresponding kinematic region does not allow to interpret this as a manifestation of coherence or a Color Glass Condensate. We demonstrate, however, that this suppression can be treated alternatively as an effective energy loss proportional to initial energy. To eliminate suppression coming from the coherence, we perform predictions for nuclear effects also at large dilepton masses. Our calculations are in a good agreement with available data. Since the kinematic limit can be also approached in transverse momenta p_T , we present in the RHIC energy range corresponding predictions for expected large- p_T suppression as well. Since a new experiment E906 planned at FNAL will provide us with more precise data soon, we present also predictions for expected large- x_F nuclear suppression in this kinematic region.

1. Introduction

In comparison with a central region of very small rapidities, $y \rightarrow 0$, the forward rapidity region allows to study processes corresponding to much higher initial energies accessible at mid rapidities. If a particle with mass M and transverse momentum p_T is produced in a hard reaction then the corresponding values of Bjorken variable in the beam and the target are $x_{1,2} = \sqrt{M^2 + p_T^2} e^{\pm y} / \sqrt{s}$. Thus, at forward rapidities the target x_2 is e^y -times smaller than at mid rapidities. This allows to study already at RHIC coherence phenomena (shadowing, Color Glass Condensate (CGC)), which are expected to suppress particle yields.

Forward rapidity physics, manifested itself as a strong nuclear suppression, has been already investigated in variety of processes at different energies: in production of different species of particles in $p + A$ collisions [1], in charge pion [2] and charmonium production [3, 4] at SPS, in the Drell-Yan process and charmonium production at Fermilab [5, 6] and later on at larger RHIC energies by measurements of high- p_T particles in $d + Au$ collisions [7, 8].

Although forward rapidity region at RHIC allows to investigate small- x coherence phenomena, one should be careful with interpretation of observed suppression. Such a suppression is arisen globally for any reaction studied so far at any energy. Namely, all fixed target experiments have too low energy for the onset of coherence effects since x_2 is not small. The rise of suppression with y (with Feynman x_F) shows the same pattern as observed at RHIC.

This universality of suppression favors also another mechanism which should be common for all reactions studied at any energy. Such a mechanism was proposed in [9] and allows to describe a strong suppression via energy conservation effects in initial state parton rescatterings. It can be also interpreted alternatively as a parton effective energy loss proportional to initial energy leading so to x_F scaling of nuclear effects.

The projectile hadron can be decomposed over different Fock states. A nucleus has a higher resolution than a proton due to multiple interactions and so can resolve higher Fock components containing more constituents. Corresponding parton distributions fall off steeper at $x \rightarrow 1$

where any hard reaction can be treated as a large rapidity gap (LRG) process where no particle is produced within rapidity interval $\Delta y = -\ln(1-x)$. The suppression factor as a survival probability for LRG was estimated in [9], $S(x) \sim 1-x$. Each of multiple interactions of projectile partons produces an extra $S(x)$ and the weight factors are given by the AGK cutting rules [10]. Then the effective parton distribution correlates with the nuclear target [9, 11],

$$f_{q/N}^{(A)}(x, Q^2, \vec{b}) = C f_{q/N}(x, Q^2) \exp\left[-[1-S(x)]\sigma_{eff}T_A(\vec{b})\right], \quad (1)$$

where $T_A(\vec{b})$ is the nuclear thickness function defined at nuclear impact parameter \vec{b} , $\sigma_{eff} = 20$ mb [9] and the normalization factor C is fixed by the Gottfried sum rule.

In this paper we study a suppression of the Drell-Yan (DY) process on a nucleus with respect to a nucleon target and the rise of this suppression with y (x_1, x_F) in various kinematic regions. First we compare our predictions with data from the fixed target E772 experiment at FNAL [5]. Then similar nuclear effects are predicted also for the RHIC forward region expecting the same suppression pattern as seen at FNAL. Finally we perform for the first time predictions in the kinematic range corresponding to a new E906 experiment planned at FNAL where no coherence effects are expected.

2. The color dipole approach

The DY process in the target rest frame can be treated as radiation of a heavy photon/dilepton by a projectile quark. The transverse momentum p_T distribution of photon bremsstrahlung in quark-nucleon interactions, $\sigma^{qN}(\alpha, \vec{p}_T)$, reads [12]:

$$\frac{d\sigma(qN \rightarrow \gamma^* X)}{d(\ln \alpha) d^2 p_T} = \frac{1}{(2\pi)^2} \sum_{in,f} \int d^2 r_1 d^2 r_2 e^{i\vec{p}_T \cdot (\vec{r}_1 - \vec{r}_2)} \Phi_{\gamma^* q}^*(\alpha, \vec{r}_1) \Phi_{\gamma^* q}(\alpha, \vec{r}_2) \Sigma(\alpha, r_1, r_2) \quad (2)$$

where $\Sigma(\alpha, r_1, r_2) = \{\sigma_{\bar{q}q}(\alpha r_1) + \sigma_{\bar{q}q}(\alpha r_2) - \sigma_{\bar{q}q}(\alpha|\vec{r}_1 - \vec{r}_2|)\}/2$, $\alpha = p_{\gamma^*}^+/p_q^+$ and the light-cone (LC) wave functions of the projectile $q + \gamma^*$ fluctuation $\Phi_{\gamma^* q}^*(\alpha, \vec{r})$ are presented in [12]. Feynman variable is given as $x_F = x_1 - x_2$ and in the target rest frame $x_1 = p_{\gamma^*}^+/p_p^+$. For the dipole cross section $\sigma_{\bar{q}q}(\alpha r)$ in Eq. (2) we used GBW [13] and KST [14] parametrizations.

The hadron cross section is given convolving the parton cross section, Eq. (2), with the corresponding parton distribution functions (PDFs) f_q and $f_{\bar{q}}$ [12, 15],

$$\frac{d\sigma(pp \rightarrow \gamma^* X)}{dx_F d^2 p_T dM^2} = \frac{\alpha_{em}}{3\pi M^2} \frac{x_1}{x_1 + x_2} \int_{x_1}^1 \frac{d\alpha}{\alpha^2} \sum_q Z_q^2 \left\{ f_q\left(\frac{x_1}{\alpha}, Q^2\right) + f_{\bar{q}}\left(\frac{x_1}{\alpha}, Q^2\right) \right\} \frac{d\sigma(qN \rightarrow \gamma^* X)}{d(\ln \alpha) d^2 p_T}, \quad (3)$$

where Z_q is the fractional quark charge, PDFs f_q and $f_{\bar{q}}$ are used with the lowest order (LO) parametrization from [16] at the scale $Q^2 = p_T^2 + (1-x_1)M^2$ and the factor $\alpha_{em}/(3\pi M^2)$ accounts for decay of the photon into a dilepton.

3. Dilepton production on nuclear targets

The rest frame of the nucleus is very convenient for study of coherence effects. The dynamics of the DY process is controlled by the coherence length,

$$l_c = \frac{2E_q \alpha(1-\alpha)}{(1-\alpha)M^2 + \alpha^2 m_q^2 + p_T^2} = \frac{1}{m_N x_2} \frac{(1-\alpha)M^2}{(1-\alpha)M^2 + m_q^2 \alpha^2 + p_T^2}, \quad (4)$$

where $E_q = x_q s/2m_N$ and m_q is the energy and mass of the projectile quark and the center of mass energy squared $s = (M^2 + p_T^2)/x_1 x_2$. The fraction of the proton momentum x_q carried by the quark is related to x_1 as $\alpha x_q = x_1$.

The coherence length is related to the longitudinal momentum transfer, $q_L = 1/l_c$, which controls the interference between amplitudes of the hard reaction occurring on different nucleons. The

condition for the onset of shadowing in a hard reaction is sufficiently **long coherence length** (LCL) in comparison with the nuclear radius, $l_c \gtrsim R_A$. Here the special advantage of the color dipole approach allows to incorporate nuclear shadowing effects via a simple eikonalization of $\sigma_{\bar{q}q}(x, r)$ [17], i.e. replacing $\sigma_{\bar{q}q}(x, r)$ in Eq. (2) by $\sigma_{\bar{q}q}^A(x, r)$:

$$\sigma_{\bar{q}q}^A = 2 \int d^2b \left\{ 1 - \left[1 - \frac{1}{2A} \sigma_{\bar{q}q} T_A(b) \right]^A \right\}. \quad (5)$$

The corresponding predictions for nuclear broadening in DY reaction based on the theory [12] for LCL limit were presented in [18].

In the **short coherence length** (SCL) regime the coherence length is shorter than the mean internucleon spacing, $l_c \lesssim 1 \div 2$ fm. In this limit there is no shadowing due to very short duration of the $\gamma^* + q$ fluctuation. The corresponding theory for description of the quark transverse momentum broadening can be found in [19, 20].

In this regime the transverse momentum distribution for an incident proton can be obtained integrating over α similarly as in Eq. (3):

$$\frac{d\sigma(pA \rightarrow \gamma^* X)}{dx_F d^2p_T dM^2} = \frac{\alpha_{em}}{3\pi M^2} \frac{x_1}{x_1 + x_2} \int_{x_1}^1 \frac{d\alpha}{\alpha^2} \sum_q Z_q^2 \left\{ f_q\left(\frac{x_1}{\alpha}, Q^2\right) + f_{\bar{q}}\left(\frac{x_1}{\alpha}, Q^2\right) \right\} \sigma^{qA}(\alpha, p_T), \quad (6)$$

where $\sigma^{qA}(\alpha, p_T)$ represents the cross section for an incident quark to produce a photon on a nucleus A with transverse momentum p_T . This cross section can be expressed convolving the probability function $W^{qA}(\vec{k}_T, x_q)$ with the cross section $\sigma^{qN}(\alpha, k_T)$ (see Eq. (2)),

$$\sigma^{qA}(\alpha, p_T) = \int d^2k_T W^{qA}(\vec{k}_T, x_q) \sigma^{qN}(\alpha, \vec{l}_T), \quad (7)$$

where $\vec{l}_T = \vec{p}_T - \alpha \vec{k}_T$.

Probability distribution in Eq. (7) that a quark will acquire transverse momentum \vec{k}_T on the nucleus, $W^{qA}(\vec{k}_T, x_q)$, is obtained by the averaging procedure over the nuclear density $\rho_A(b, z)$:

$$W^{qA}(\vec{k}_T, x_q) = \frac{1}{A} \int d^2b dz \rho_A(b, z) W_A^q(\vec{k}_T, x_q, \vec{b}, z), \quad (8)$$

where $W_A^q(\vec{k}_T, x_q, \vec{b}, z) = dn_q/d^2k_T$ means now the partial probability distribution that a valence quark arriving at the position (\vec{b}, z) in the nucleus A will have acquired transverse momentum \vec{k}_T . It can be written in term of the quark density matrix, $\Omega_q(\vec{r}_1, \vec{r}_2) = (b_0^2/\pi) \exp(-b_0^2(r_1^2 + r_2^2)/2)$,

$$W_A^q(\vec{k}_T, x_q, \vec{b}, z) = \frac{1}{(2\pi)^2} \int d^2r_1 d^2r_2 e^{i\vec{k}_T \cdot (\vec{r}_1 - \vec{r}_2)} \Omega_q(\vec{r}_1, \vec{r}_2) e^{-\frac{1}{2} \sigma_{\bar{q}q}(x_q, \vec{r}_1 - \vec{r}_2) T_A(\frac{\vec{r}_1 + \vec{r}_2}{2} + \vec{b}, z)}, \quad (9)$$

where $b_0^2 = \frac{2}{3\langle r_{ch}^2 \rangle}$ with $\langle r_{ch}^2 \rangle = 0.79 \pm 0.03$ fm² representing the mean-square charge radius of the proton. $T_A(b, z)$ in Eq. (9) is the partial nuclear thickness function, $T_A(b, z) = \int_{-\infty}^z dz' \rho_A(b, z')$.

Nuclear effects in $p+A$ collisions are usually investigated via the so called nuclear modification factor, defined as $R_A(p_T, x_F, M) = \frac{d\sigma(pA \rightarrow \gamma^* X)}{dx_F d^2p_T dM^2} / A \frac{d\sigma(pN \rightarrow \gamma^* X)}{dx_F d^2p_T dM^2}$, where the numerator is calculated in SCL and LCL regimes as described above. Corrections for the finite coherence length was realized by linear interpolation using nuclear longitudinal formfactor [21] (for more sophisticated Green function method see [12, 22]).

Note that at RHIC energy and at forward rapidities the eikonal formula for LCL regime, Eqs. (3) and (5), is not exact since higher Fock components containing gluons lead to additional corrections, called gluon shadowing (GS). The corresponding suppression factor R_G was derived in [21, 18] and included in calculations replacing in Eq. (5) $\sigma_{\bar{q}q}$ by $R_G \sigma_{\bar{q}q}$. GS leads to reduction of the Cronin effect [23] at medium-high p_T and to additional suppression (see Fig. 3).

In the fixed target FNAL energy range, for elimination of the coherence effects one can study production of dileptons at large M (see Eq. (4)) as has been realized by the E772 Collaboration [5]. Another possibility is to study the DY process at large $x_1 \rightarrow 1$, when also $\alpha \rightarrow 1$, and $l_c \rightarrow 0$ in this limit (see Eq. (4)).

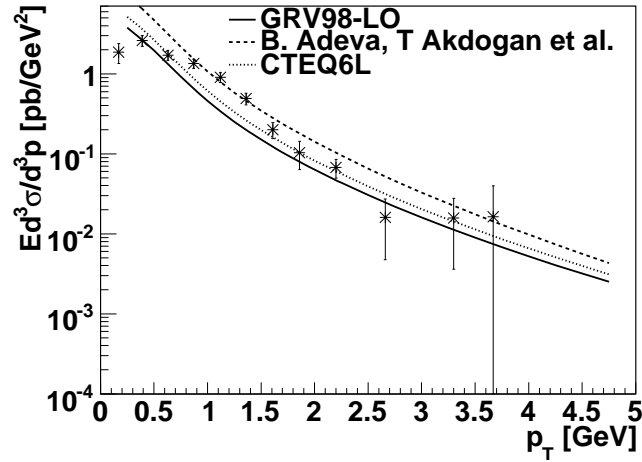


Figure 1. Differential cross section of dileptons in $p + p$ collisions at $x_F = 0.63$ and $M = 4.8$ GeV vs. E866 data [24].

4. Nuclear suppression at forward rapidities: model vs. data

We start with the DY process in $p + p$ collisions. Besides calculations based on Eq. (3) using GRV98 PDFs [16] (see the solid line in Fig. 1) we present by the dashed and dotted line also predictions using proton structure functions from [25] and CTEQ6L parametrization of PDFs from [26], respectively. Fig. 1 shows a reasonable agreement of the model with data from the E866/NuSea Collaboration [24]. This encourages us to apply the color dipole approach to nuclear targets as well.

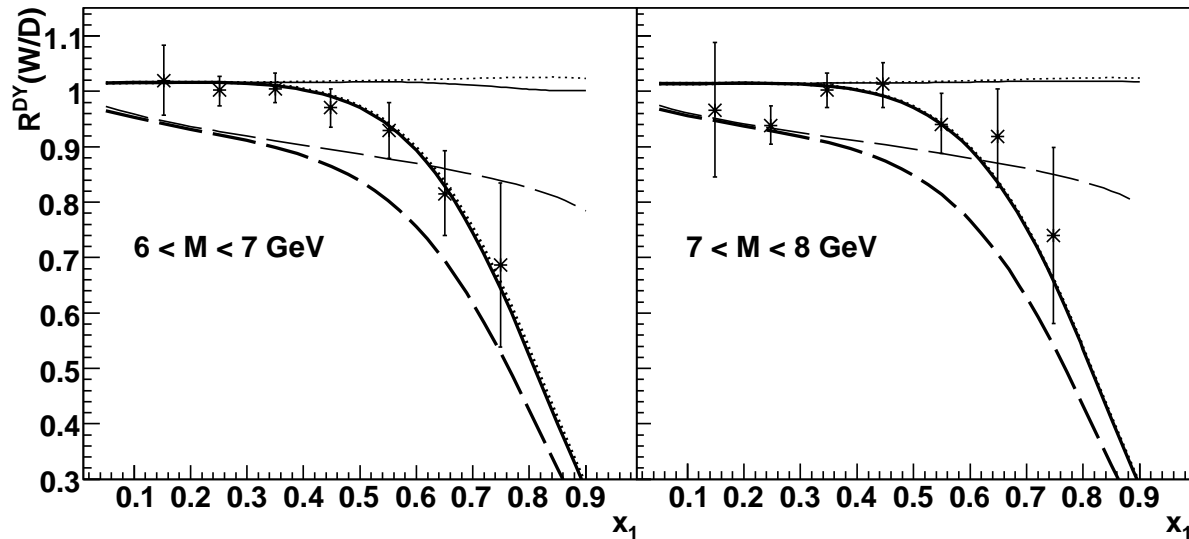


Figure 2. Ratio $R^{DY}(W/D)$ of Drell-Yan cross sections on W and D vs. E772 data for $6 < M < 7$ GeV (Left) and $7 < M < 8$ GeV (Right). Predictions correspond to SCL (dotted curves), LCL (dashed curves) regimes and their interpolation (solid curves). Thick and thin curves are calculated with and without corrections (1) for energy conservation, respectively.

The E772 Collaboration [5] found a significant suppression of DY pairs at large x_1 (see Fig. 2). Large invariant masses of the photon allows to minimize shadowing effects (see a small differences between dotted and solid lines in Fig. 2). If effects of energy conservation, Eq. (1), are not included one can not describe a strong suppression at large x_1 . In the opposite case a reasonable agreement of our model with data is achieved.

One can approach the kinematic limit increasing p_T . Therefore we present also predictions for p_T dependence of the nuclear modification factor R_{d+Au} at RHIC energy and at several fixed values of x_F . Similarly as in [9] instead of usual Cronin enhancement, a suppression is found (see Fig. 3). The onset of isotopic effects (IE) in $d + Au$ collisions at large p_T gives the values $R_{d+Au}^{IE} \sim 0.73 \div 0.79$ depending on x_F . In $p + Au$ collisions the corresponding ratio $R_{p+Au} \rightarrow 1$ from above and no nuclear effects are assumed at large p_T expecting so QCD factorization. However, we predict a strong onset of effective energy loss effects, Eq. (1), at large x_F (see Fig. 3) quantifying itself as a large deviation of suppression from the above values R_{d+Au}^{IE} . The predicted huge rise of suppression with x_F in Fig. 3 reflects much smaller survival probability $S(x_F)$ at larger x_F and can be tested in the future by the new data from RHIC. Note that effects of GS depicted in Fig. 3 by the thick lines lead to additional suppression which rises with x_F .

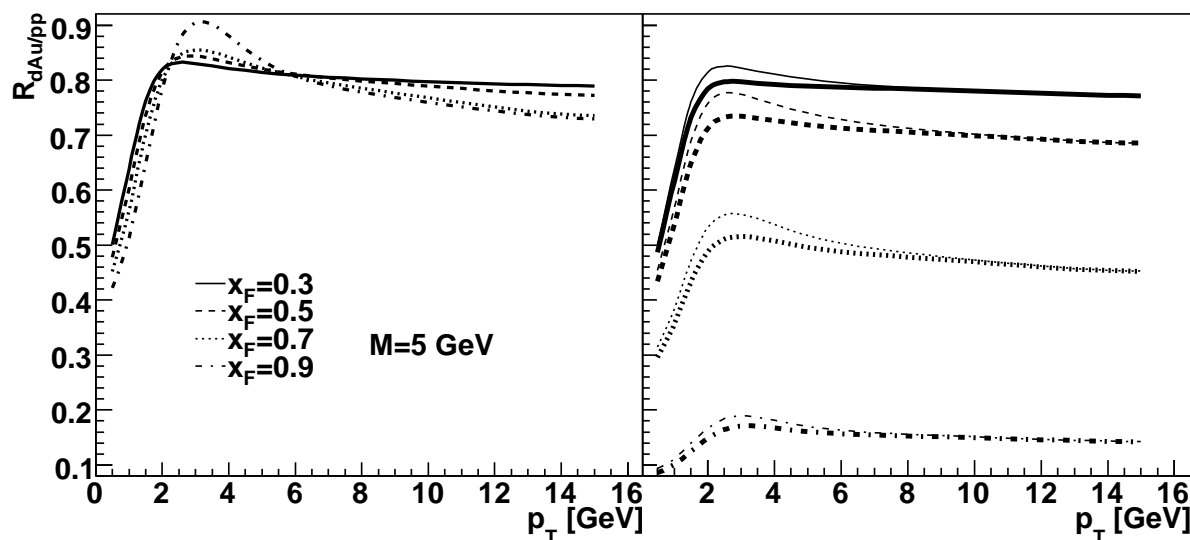


Figure 3. (Left) Predictions for the ratio $R_{d+Au}(p_T)$ at $\sqrt{s} = 200$ GeV for several fixed values of x_F without effects of effective energy loss. (Right) The same as (Left) but with effects of effective energy loss, Eq. (1), (thin lines). Thick lines additionally include GS effects.

Finally we present in Fig. 4 for the first time predictions for x_1 dependence of the nucleus-to-nucleon ratio in the kinematic range corresponding to a new E906 experiment planned at Fermilab. We should not expect any shadowing effects since initial energy is small, $E_{lab} = 120$ GeV and a strong nuclear suppression at large x_1 is caused predominantly by the energy conservation constraints, Eq. (1).

5. Summary

We demonstrate that besides an onset of coherence a nuclear suppression at forward rapidities (large x_1 , x_F) can be induced also by energy conservation effects in multiple parton rescatterings interpreted alternatively as a parton effective energy loss proportional to initial energy. Universality of this treatment is in its applicability to any reaction studied at any energy also in the kinematic regions where coherence phenomena (shadowing, CGC) can not be manifested. First we apply this approach to the DY process and explain well a significant suppression at large x_1 in accordance with the E772 data. The FNAL energy range and large invariant masses of the photon allow to minimize the effects of coherence, what does not leave much room for other mechanisms, such as CGC. Then we predict a significant suppression also for $d + Au$ collisions at RHIC in the forward region (see Fig. 3). At small p_T we show an importance of GS effects and their rise with x_F . Finally we present for the first time predictions for strong nuclear effects expected in a new E906 experiment planned at FNAL. Much smaller beam energy than in E772 experiment allows to exclude safely interpretations based on coherence phenomena.

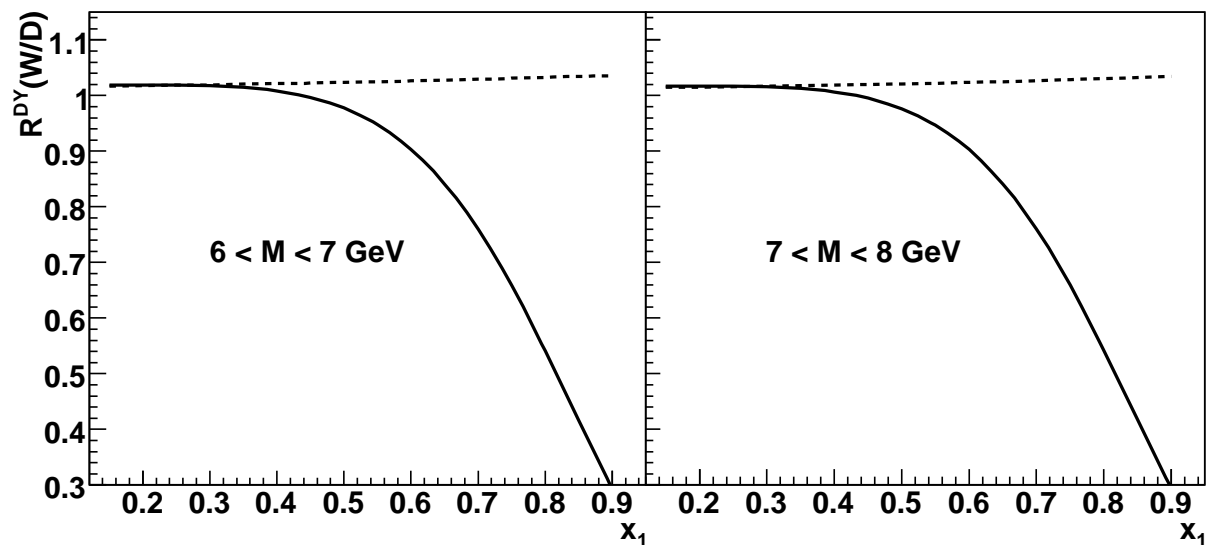


Figure 4. (Left) Predictions for the ratio $R^{DY}(W/D)$ of Drell-Yan cross sections on W and D for $6 < M < 7$ GeV (Left) and $7 < M < 8$ GeV (Right) realized for the kinematic range of the planned E906 experiment at Fermilab. Solid and dashed curves are calculated with and without effects of effective energy loss, Eq. (1), respectively.

Acknowledgments

This work was supported in part by the Slovak Funding Agency, Grant 2/0092/10 and by Grants VZ MŠMT 6840770039 and LC 07048 (Ministry of Education of the Czech Republic).

References

- [1] Barton D S, et al. 1983 *Phys. Rev. D* **27** 2580; Geist W M 1991 *Nucl. Phys. A* **525** 149c; Beretvas A, et al. 1986 *ibid.* **34** 53; Binkley M, et al. 1976 *Phys. Rev. Lett.* **37** 571; Bailey R, et al. 1984 *Z. Phys. C* **22** 125; Skubic P, et al. 1978 *Phys. Rev. D* **18** 3115
- [2] NA49 Collaboration, Boimska B 2004 *Ph.D. Dissertation* (Warsaw 2004) **CERN-THESIS-2004-035**
- [3] NA3 Collaboration, Badier J, et al. 1983 *Z. Phys. C* **20** 101
- [4] NA38 Collaboration, Abreu M C, et al. 1999 *Phys. Lett. B* **449** 128
- [5] E772 Collaboration, Alde D M, et al. 1990 *Phys. Rev. Lett.* **64** 2479
- [6] E866 Collaboration, Leitch M J, et al. 2000 *Phys. Rev. Lett.* **84** 3256
- [7] BRAHMS Collaboration, Arsene I, et al. 2004 *Phys. Rev. Lett.* **93** 242303; Hongyan Yang, et al. 2007 *J. Phys. G* **34** S619
- [8] STAR Collaboration, Adams J, et al. 2006 *Phys. Rev. Lett.* **97** 152302
- [9] Kopeliovich B Z, et al. 2005 *Phys. Rev. C* **72** 054606; Nemchik J, et al. 2008 *Phys. Rev. C* **78** 025213
- [10] Abramovsky A V, Gribov V N and Kancheli O V 1973 *Yad. Fiz.* **18** 595
- [11] Kopeliovich B Z and Nemchik J 2010 *preprint arXiv:1009.1162*[hep-ph]
- [12] Kopeliovich B Z, Schäfer A and Tarasov A V 1999 *Phys. Rev. C* **59** 1609
- [13] Kowalski H, Motyka L and Watt G 2006 *Phys. Rev. D* **74** 074016
- [14] Kopeliovich B Z, Schäfer A and Tarasov A V 2000 *Phys. Rev. D* **62** 054022
- [15] Kopeliovich B Z, Raufeisen J and Tarasov A V 2001 *Phys. Lett. B* **503** 91
- [16] Gluck M, Reya E and Vogt A 1998 *Eur. Phys. J. C* **5** 461
- [17] Zamolodchikov A B, Kopeliovich B Z and Lapidus L I 1981 *Sov. Phys. JETP Lett.* **33** 595
- [18] Kopeliovich B Z, et al. 2003 *Phys. Rev. C* **67** 014903
- [19] Johnson M B, Kopeliovich B Z and Tarasov A V 2001 *Phys. Rev. C* **63** 035203
- [20] Johnson M B, Kopeliovich B Z and Schmidt I 2007 *Phys. Rev. C* **75** 064905
- [21] Kopeliovich B Z, Nemchik J, Schäfer A and Tarasov A V 2002 *Phys. Rev. C* **65** 035201
- [22] Nemchik J 2003 *Phys. Rev. C* **68** 035206
- [23] Kopeliovich B Z, Nemchik J, Schäfer A and Tarasov A V 2002 *Phys. Rev. Lett.* **88** 232303
- [24] E886/NuSea Collaboration, Webb J C, et al. 2003 *preprint arXiv:hep-ex/0302019*; Webb J C 2002 **FERMILAB -THESIS-2002-56** (*Preprint hep-ex-0301031*)
- [25] SMC Collaboration, Adeva B, et al. 1998 *Phys. Rev. D* **58** 112001
- [26] Pumplin J, Stump D R, Huston J, Lai H L, Nadolsky P and Tung W K 2002 *JHEP* **0207** 012